

# Chapter 10

## Reliability Quantification of High-Speed Naval Vessels Based on SHM Data

Mohamed Soliman and Dan M. Frangopol

**Abstract** Identification of the structural responses of high-speed naval vessels under normal sea operation is subjected to uncertainties associated with the loading conditions, material properties, cross-sectional dimensions and damage propagation, among others. Probabilistic analyses provide appropriate performance indicators, such as the reliability index, which can simultaneously consider these uncertainties in the prediction of the service life of ships based on the required reliability levels. In this context, structural health monitoring (SHM) can aid in determining the seaway loading conditions and quantifying the structural responses under different operational conditions. As a result, uncertainties associated with the performance prediction can be quantified and some of them (i.e., epistemic uncertainties) can be reduced. In this paper, reliability assessment, based on SHM data, of high-speed naval vessels is performed. Information from SHM is used to estimate the actual structural response associated with the sea states, ship speeds, and wave headings encountered by the vessel. Recorded structural responses are used to establish the time-variant performance profile of the studied cross-sections. This profile can be used to predict the remaining service life and to plan for the appropriate threshold-based inspections and repair actions. The presented approach is applied to a high speed naval vessel.

**Keywords** Structural health monitoring • Uncertainty • Naval vessel • Deterioration • Reliability

### 10.1 Introduction

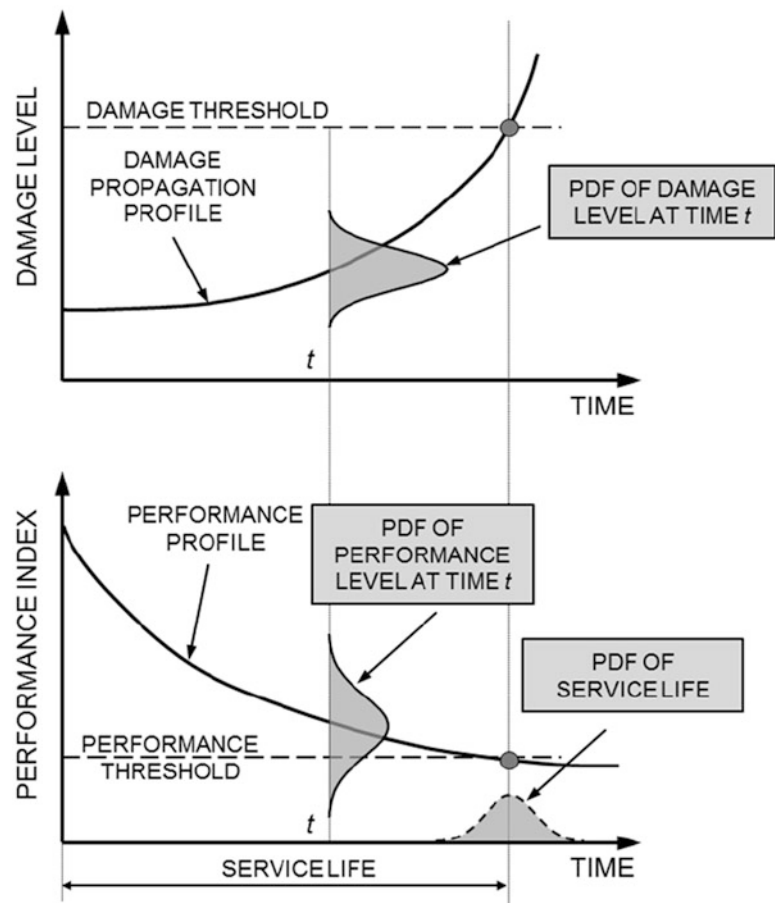
Evaluation of the performance of ships under normal operational conditions is usually a demanding task. This is mainly due to the presence of uncertainties associated with the sea loading conditions, material properties, and damage initiation and propagation, among others [1, 2]. This is especially true for high-speed aluminum vessels. In these ships, to comply with the speed and load requirements, the designers and manufacturers usually use innovative structural details whose behavior may not be fully understood [3]. As a result, more research is still needed for evaluating the structural performance of high-speed naval vessels. Aluminum naval vessels are subjected to various time-dependent structural deterioration mechanisms such as fatigue and corrosion [4]. Fatigue is one of the most critical deteriorating mechanisms. It occurs at locations with high stress concentration or fabrication defects. Stress fluctuations at these locations during ship operation may cause cracks to initiate and propagate. These cracks, if not inspected and repaired in a timely manner, may cause fracture of the affected components and may lead to catastrophic failures. Corrosion losses, on the other hand, may cause reduction in the hull structural resistance, reduction in the local strength, and/or increase in the fatigue crack propagation rate within the damaged area. Aluminum vessels generally have high corrosion resistance due to the formation of a thin oxide layer which prevents any further corrosion to the core metal. However, aluminum is prone to galvanic corrosion if not properly isolated.

Due to these deterioration effects, the structural performance degrades with time as shown in Fig. 10.1. Additionally, due to the aforementioned uncertainties, the predicted structural performance carries inherent uncertainty. Therefore, the performance assessment process must be handled probabilistically [5–7].

---

M. Soliman (✉) • D.M. Frangopol  
Department of Civil and Environmental Engineering, ATLSS Engineering Research Center, Lehigh University,  
117 ATLSS Drive, Bethlehem, PA 18015-4729, USA  
e-mail: [mos209@lehigh.edu](mailto:mos209@lehigh.edu); [dan.frangopol@lehigh.edu](mailto:dan.frangopol@lehigh.edu)

**Fig. 10.1** Time-variant damage level and performance under uncertainty



As shown in Fig. 10.1, there is an inherent uncertainty in the damage level as well as the performance level at any time. These uncertainties affect the service life estimation under deterioration effects. In this context, structural health monitoring (SHM) can be used to increase the accuracy of the performance prediction process by providing an insight into the structural responses under normal operational conditions.

For high-speed naval vessels, analysis should be performed to ensure the adequacy of the structural design under normal operational loading. This analysis requires a detailed full-scale three-dimensional finite element model where the critical loading is determined from seakeeping trials or testing. The load effects arising from such trials are applied to the model and the performance, in terms of the maximum stress, is checked against allowable limits. While performing such analyses, only the worst loading condition is selected for structural performance checks; however, this value of the maximum load effect carries significant variability and may not be a realistic representation of the normal sea operational conditions. Therefore, a systematic method for the performance evaluation that can account for this variability is required. Furthermore, an approach for quantifying this uncertainty is also essential. In this context, structural reliability index can be used as a performance indicator which integrates the uncertainties associated with the load effects and the structural resistance. Additionally, the inclusion of structural health monitoring information during ship operation can be used to quantify such uncertainties, especially those associated with the load effects. Similarly, for assessing the fatigue performance of structural details in ships, it is usually very difficult to find an accurate estimation of the stress range distribution under a given sea condition; a process that may consist of significant uncertainties and approximations when performed using traditional approaches, such as the spectral fatigue approach. Thus, the use of structural health monitoring information can also assist in quantifying the uncertainties and establishing an accurate prediction of the time-variant fatigue performance at critical details.

In this paper, an approach for predicting the structural reliability of naval vessels based on SHM information under a given operational condition is presented. The approach uses the SHM data collected during seakeeping trials to find an estimate of the load effects and uses system reliability concepts to compute the time-variant structural reliability of a given frame under the effects of global bending and fatigue damage. The presented approach is applied to the reliability evaluation of an existing aluminum high-speed naval vessel.

## 10.2 Structural Reliability

Probability of failure and the reliability index are among the widely used probabilistic performance indicators for the life-cycle assessment. The probability of system failure is defined as the probability of violating any of the limit states that define its failure modes. A limit-state consisting of the capacity and demand terms representing the structural resistance,  $R(t)$ , and load effects,  $S(t)$ , respectively, is defined as

$$g(t) = R(t) - S(t) = 0 \quad (10.1)$$

where  $R(t)$  and  $S(t)$  are expressed in terms of the governing random variables (e.g., yield stress, load effects, and parameters of the deterioration model) at time  $t$ . The corresponding time-variant reliability index  $\beta(t)$  can be computed as

$$\beta(t) = \Phi^{-1}(1 - P_f(t)) \quad (10.2)$$

where  $\Phi(\cdot)$  is the cumulative distribution function of standard normal distribution. The reliability index is generally decreasing with time due to various environmental and mechanical stressors (see Fig. 10.1).

In this paper, two modes of failure are considered for the reliability analyses. The effect of the global longitudinal bending moment (i.e., global failure mode) is considered as the first failure mode, while the second failure mode is the fatigue failure due to stress fluctuation at critical locations. For the first mode, since the longitudinal bending moment acts in sagging and hogging, the reliability of the ship structure, at the monitored locations, associated with this failure mode is computed in terms of the induced strain in both sagging and hogging. In this mode, the strains induced due to slamming and whipping can be taken into account. The limit state  $g$  associated with the sagging or hogging in this failure mode is defined as [8]

$$g = x_R \varepsilon_R - x_w (\varepsilon_w + k_d \varepsilon_d) = 0 \quad (10.3)$$

where  $\varepsilon_R$  is the resisting strain,  $\varepsilon_w$  and  $\varepsilon_d$  are the strains produced by the wave induced bending moment and the dynamic load effects, respectively.  $x_R$  and  $x_w$  are the model uncertainty parameters associated with the resisting strain and the wave-induced strains, respectively.  $k_d$  represents the correlation factor between the wave-induced moment and the dynamic load effects. The strains  $\varepsilon_R$  and  $\varepsilon_d$  can be effectively recorded and acquired using an onboard SHM system.

Fatigue, as the second mode of failure, is one of the main stressors which can induce structural damage in ships [7]. Fatigue damage can occur at regions of weld defects, stress concentrations, or discontinuities [9]. Environmental effects such as corrosion may increase the fatigue effects at the damaged area [10]. Currently, the  $S-N$  (i.e., stress-life) approach is widely used for fatigue life estimation of ships. In this approach, fatigue life of a detail is determined based on the relationship between the stress range acting on the detail and the number of cycles to failure. This relationship is established through the laboratory testing of similar details subjected to different stress range values and analyzing the corresponding cycles to failure. Various design guides and standards (e.g. [11, 12]) provide the  $S-N$  relationships for multiple classes (or categories) of details. The  $S-N$  relationship is given as

$$S = \left( \frac{A}{N} \right)^{\frac{1}{m}} \quad (10.4)$$

where  $S$  is the stress range,  $A$  and  $m$  are the  $S-N$  category coefficients, and  $N$  is the number of cycles. Various approaches may be used to define the stress range acting on the detail; namely, the nominal stress, the hot-spot stress, and the notch stress [13]. The selection of the stress range definition depends on the specifications adopted to calculate the fatigue life in addition to the method used to estimate the actual stress range affecting the detail. Miner's rule can be used to estimate the cumulative fatigue damage assuming that damage at any particular stress range level is a linear function of the corresponding number of cycles to failure. Thus, Miner's damage index  $D$  is expressed as [14]

$$D = \sum_{i=1}^n \frac{n_i}{N_i} \quad (10.5)$$

where  $n_i$  is the number of cycles at the  $i$ th stress and  $N_i$  is the number of cycles to failure under the same stress range. Using this approach, the failure at a detail is expected to occur when the damage index reaches one. However, this value carries

significant variability [15, 16]. Since ship details are normally subjected to variable amplitude stress ranges arising from the sea loading, an equivalent constant amplitude stress range  $S_{re}$  is found as [4]

$$S_{re} = \left( \sum \frac{n_i}{N_i} S_{ri}^m \right)^{\frac{1}{m}} \quad (10.6)$$

where  $S_{ri}$  is the stress range of the  $i$ th bin in the stress range histogram. In this paper, the stress range bin histograms under different sea operational conditions are established based on the strains recorded during the SHM of the ship. Based on the stress range data and the fatigue resistance of the analyzed structural detail, a fatigue limit state can be defined as

$$g(t) = \Delta - D(t) = 0 \quad (10.7)$$

where  $\Delta$  is Miner's critical damage accumulation index representing the resistance and  $D(t)$  is the time-dependent damage accumulation index resulting from sea loading.  $D(t)$  is a function of the  $S$ - $N$  parameters (i.e.,  $A$  and  $m$ ) as well as the stress range and number of cycles resulting from the sea operation. After defining the random variables and deterministic parameters associated with the limit states considered, the probability of failure (i.e., violating the limit state) and the reliability index can be found using specialized reliability software such as CalREL [17], or by using probabilistic simulation methods. In this paper, the software CalREL is used to compute the reliability index and the probability of failure.

### 10.3 Analysis of SHM Data

In general, the load effects recorded by the SHM system consist of both wave induced and slam induced effects. Therefore, the collected signal consists of high- and low-frequency components produced by slamming effects and wave-induced bending moments, respectively. The SHM information is treated differently for evaluating the fatigue and global bending reliability. For global bending, the recorded load effects are digitally filtered to separately study the contribution of the wave-induced and slam-induced bending moment effects. However, for fatigue reliability evaluation, the entire combined record is used to build the stress range bin histograms. For evaluating the global bending reliability, digital filters are used to find the contribution of the wave-induced and slam-induced effects separately. Next, peak extraction is employed to find the peak strains from the record of the SHM signal. As reported in [8], low- and high-frequency peak distributions follow the Rayleigh and exponential distributions, respectively. Since the reliability with respect to the global bending should be performed with respect to the extreme events, extreme value analyses are considered for the load effects, and the parameters of Type I distribution, which represents the form to which both the Rayleigh and exponential distributions asymptotically converge, are identified.

### 10.4 Illustrative Example

The reliability evaluation approach discussed in this paper is applied to the HSV-2 swift, an aluminum high-speed wave piercing catamaran with an overall length of 98 m. As indicated in [18–20], the ship was completed in 2003 and was instrumented and tested to measure the primary load responses, stress concentrations, and secondary slam loads, among others. Strain gages were wired and connected to remote junction boxes and an instrumentation trailer. A total of 16 sensors (denoted T1 sensors) were installed to record the global structural behavior covering bending stresses, pitch connecting moments and split. Additionally, 19 sensors were installed at various locations to measure the stress concentration (denoted T2 sensors). In this paper, the signals of two sensors installed on Frame 26 of the ship are analyzed. The first sensor is T1-8 which measures the global bending response and the second is T2-5 which measures the local bending stresses at the keel at Frame 26. The stress signals recorded at T1-8 are used herein to find the global bending reliability of Frame 26 while those of T2-5 are used to study its fatigue reliability. The location of the two sensors within the ship is shown in Fig. 10.2.

For evaluating the global bending reliability, the signal record of T1-8 is studied and a digital filter is applied to isolate the effects of wave induced bending moment and slam induced bending effects. After analyzing the power spectra of signals recorded during various operational conditions, a cut-off frequency of 1.0 Hz was selected and a Butterworth filter was applied to find the separate effects of both actions. In Fig. 10.3a, the amplitudes of the Fourier transform of one strain signal recorded at head sea condition at speed 15 knots and sea state 5 are shown. On the other hand, for analyzing the fatigue reliability, since both the low- and high-frequency stress cycles contribute to the fatigue damage accumulation it was not

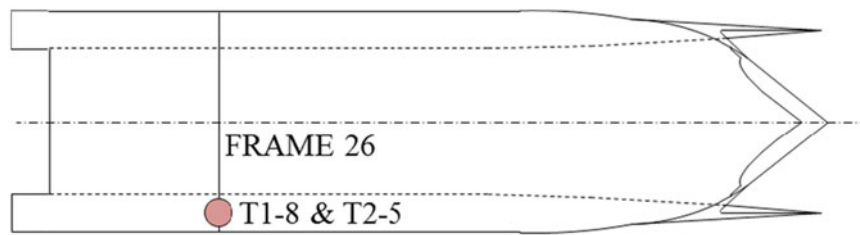


Fig. 10.2 Plan view of the ship showing the location of the analyzed sensors (based on [18–20])

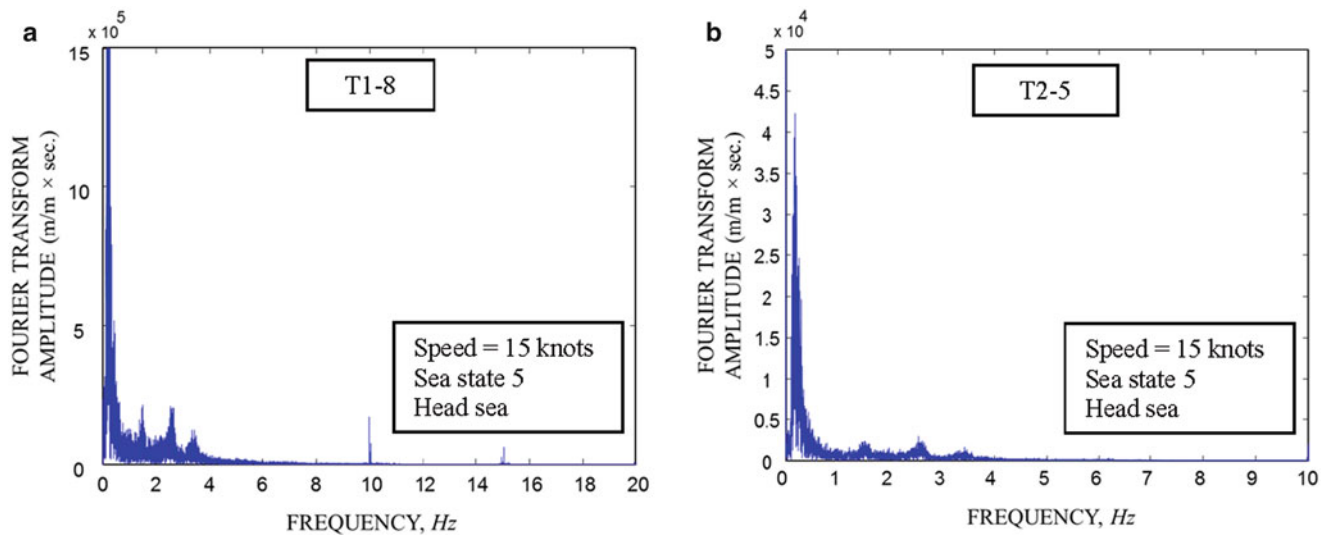


Fig. 10.3 Amplitudes of the Fourier transform of strain signals; (a) sensor T1-8, and (b) sensor T2-5

necessary to identify the low- and high-frequency strain components. However, a digital low-pass Butterworth filter was applied to remove low-amplitude stress cycles associated with very high frequencies induced by external noise. Additionally, after analyzing strain signals at various operational conditions (see Fig. 10.3b), it was found that the amplitudes become negligible for frequencies larger than 7.0 Hz. Thus, it was selected as the cut-off frequency for fatigue damage reliability analysis.

After acquiring the low- and high-frequency strain records for the global bending sensors, a peak extraction algorithm is used to find the positive datasets of peaks for sagging (i.e., positive peaks) and hogging (i.e., negative peaks) effects. Next, the histograms of the obtained low- and high-frequency components are built and a distribution fitting is performed. As indicated in [8], the Rayleigh distribution provides the best fit for the low-frequency peaks while the exponential distribution provides the best fit for the high-frequency peaks. Using the parameters of the fitted distributions, extreme value statistics are used to find the corresponding parameters of the Type I distribution which are, in turn, used to evaluate the global bending reliability.

Fatigue damage accumulation is performed in this example by using the hot-spot stress approach. The hot-spot parameters proposed in [16] are used herein. Table 10.1 shows the values of various parameters used in the reliability evaluation. The ship operational rate is considered to be 2/3 (i.e., the ship operates only 2/3 of the time). After analyzing the strain signal, the rainflow algorithm [21] is used, under the assumption of linear behavior, to construct the stress range histograms for each operational condition. The resulting histograms are used to find the equivalent stress range and the average number of cycles for each operational state. Figure 10.4 shows the general flowchart for the reliability evaluation approach proposed in this paper.

At this stage, all the information related to the limit state functions given by Eqs. 10.3 and 10.7 is obtained. Three failure modes are considered as follows: (a) global sagging bending failure (Eq. 10.3), (b) global hogging bending failure (Eq. 10.3), and (c) fatigue failure (Eq. 10.7). A series system consisting of the three failure modes is constructed and the time-variant reliability index of this system is found using the CalREL software [17].

Figure 10.5 shows the time-variant system reliability index obtained for the analyzed frame at various speeds for sea state 5 and head sea conditions. As expected, the reliability index of the ship is significantly affected by the navigation speed.

**Table 10.1** Deterministic parameters and random variables for reliability assessment

Parameter	Distribution type	Mean value	COV <sup>a</sup>
$x_R^b$	Normal	1.0	0.1
$x_w^b$	Normal	0.9	0.15
$\varepsilon_R$ ( $\mu\text{m/m}$ ) <sup>b</sup>	Lognormal	870	0.1
$\varepsilon_w, \varepsilon_d$ ( $\mu\text{m/m}$ )	Type I extreme value	SHM data	SHM data
$k_d^b$	–	1.0	–
$m^c$	–	3.0	–
$\Delta^c$	Lognormal	1.0	0.48
$S_{re}$ (MPa)	Lognormal	SHM data	0.1
$mean(\log A)$	Lognormal	11.47	0.53

<sup>a</sup>Coefficient of variation

<sup>b</sup>Based on [8]

<sup>c</sup>Based on [16]

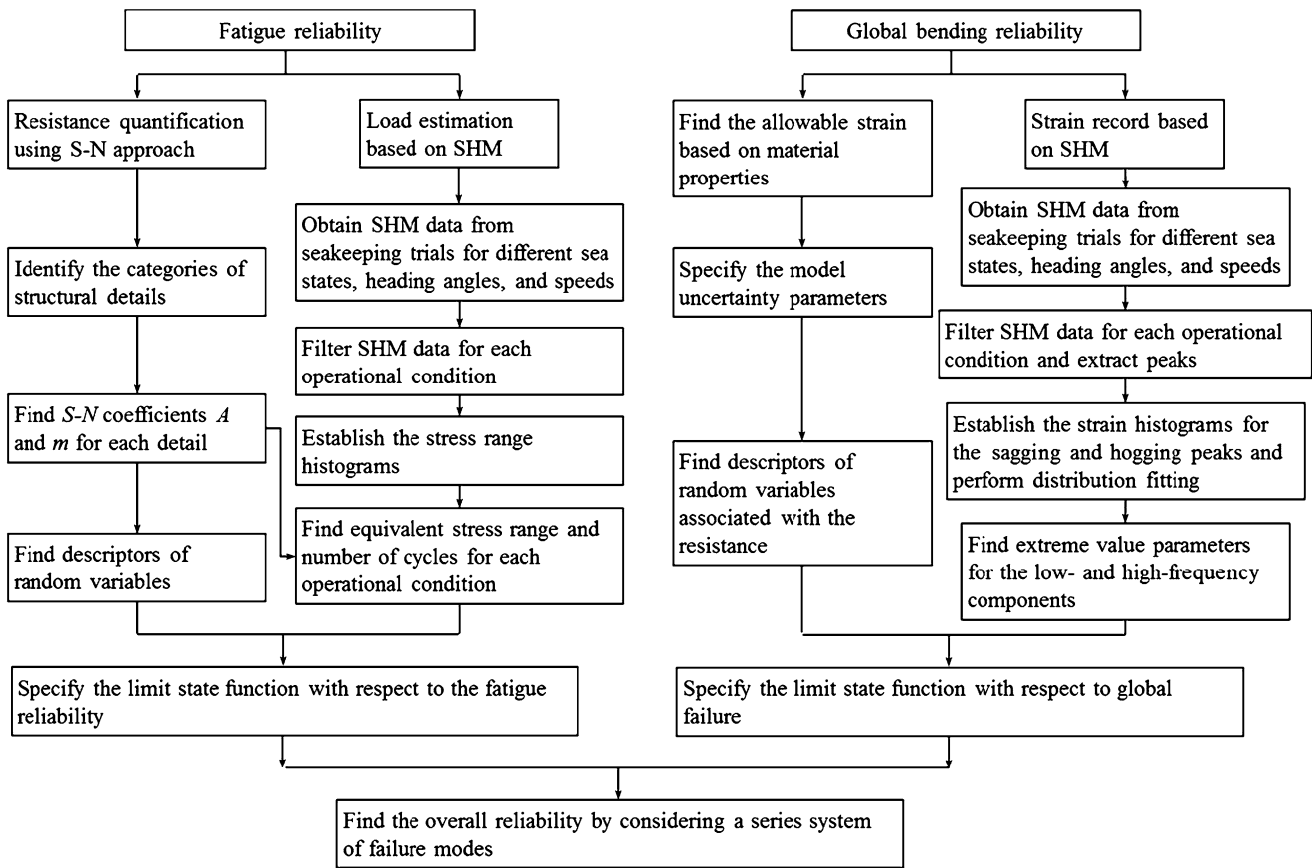


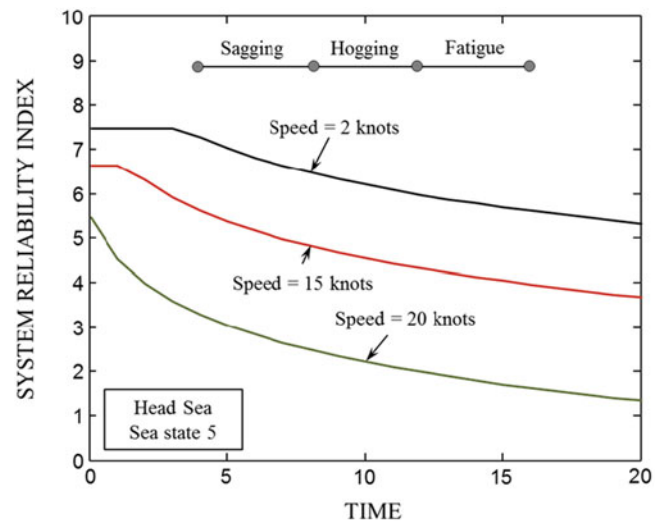
**Fig. 10.4** Flowchart for the structural reliability evaluation under the global and fatigue failure

It is also found that at low speeds, the reliability index with respect to the global bending failure may be less than that of the fatigue failure, especially early in the service life of the ship. It is also observed through investigating the results that the sagging and hogging failure modes provide very close reliability values for the analyzed frame.

### 10.5 Conclusions

This paper presented an approach for evaluating the reliability of high-speed naval vessels with respect to fatigue and global bending failure. In the studied frame, a series system of the considered failure modes is constructed and its reliability index profile is obtained. SHM data were used to find an accurate estimate of the load effects generated on the ship during normal sea operation. For analyzing the global bending response of the ship, low- and high-frequency components of the strain signal

**Fig. 10.5** Time-variant system reliability index at various speeds considering sagging, hogging, and fatigue failure



are identified and a peak extraction algorithm is applied to find the histograms of the strain peaks for sagging and hogging. Extreme value statistics are used to find the parameters of the extreme value distribution of the global effects. For fatigue reliability evaluation, the stress range bin histograms were built using the SHM data to provide an estimate of the equivalent stress range and the average number of cycles of the detail at a given sea condition. The methodology was illustrated on the naval HSV-2 strain data obtained from the SHM information recorded during the seakeeping trials of the ship. As expected, it was shown that the speed of the ship significantly affects the reliability. It was also observed that fatigue becomes the dominant failure mode after few years of the service life. This number of years can be clearly found by plotting the reliability index profiles. Using these profiles and by setting the appropriate threshold, the reliability-based service life can be obtained. Furthermore, an integrated approach can be used to evaluate the overall ship reliability under its full expected operational profile. The approach presented in this paper reveals the advantages of using SHM information for quantifying uncertainties associated with the performance evaluation of ship structures.

**Acknowledgements** The support of the U.S. Office of Naval Research (Awards numbers N00014-08-1-0188 and N00014-12-1-0023, Structural Reliability Program, Director Dr. Paul E. Hess III, ONR, Code 331) is gratefully acknowledged. The opinions and conclusions presented in this paper are those of the writers and do not necessarily reflect the views of the sponsoring organization.

## References

1. Kwon K, Frangopol DM (2012) Fatigue life assessment and lifetime management of aluminum ships using life-cycle optimization. *J Ship Res* 56:91–105
2. Frangopol DM, Bocchini P, Deco A, Kim S, Kwon K, Okasha NM, Saydam D (2012) Integrated life-cycle framework for maintenance, monitoring, and reliability of naval ship structures. *Nav Eng J* 124(1):89–99
3. Salvino LW, Brady TF (2008) Hull monitoring system development using hierarchical framework for data and information management. In: Proceedings of the 7th international conference on computer and IT applications in the maritime industry
4. Kwon K, Frangopol DM, Kim S (2013) Fatigue performance assessment and lifetime prediction of high-speed ship structures based on probabilistic lifetime sea loads. *Struct Infrastruct Eng* 9:102–115
5. Frangopol DM (2011) Life-cycle performance, management, and optimization of structural systems under uncertainty: accomplishments and challenges. *Struct Infrastruct Eng* 7:389–413
6. Kim S, Frangopol DM, Soliman M (2013) Generalized probabilistic framework for optimum inspection and maintenance planning. *J Struct Eng* 139:435–447
7. Kim S, Frangopol DM (2011) Optimum inspection planning for minimizing fatigue damage detection delay of ship hull structures. *Int J Fatigue* 33:448–459
8. Okasha NM, Frangopol DM, Saydam D, Salvino LW (2011) Reliability analysis and damage detection in high-speed naval craft based on structural health monitoring data. *Struct Health Monit* 10:361–379
9. Fisher JW (1984) *Fatigue and fracture in steel bridges, case studies*. Wiley, New York
10. Barsom JM, Rolfe ST (1999) *Fracture and fatigue control in structures: applications of fracture mechanics*. ASTM International, West Conshohocken, PA
11. Eurocode 3 (2010) Design of steel structures part 1–9, fatigue strength. CEN—European committee for Standardisation

12. Eurocode 9 (2009) Design of aluminium structures part 1–3, additional rules for structures susceptible to fatigue. CEN—European committee for Standardisation
13. Ye N, Moan T (2002) Fatigue and static behaviour of aluminium box-stiffener lap joints. *Int J Fatigue* 24:581–589
14. Miner MA (1945) Cumulative damage in fatigue. *J Appl Mech* 12:159–164
15. Ayyub BM, Assakkaf IA, Kihl DP, Siev MW (2002) Reliability-based design guidelines for fatigue of ship structures. *Nav Eng J* 114:113–138
16. Collette M, Incecik A (2006) An approach for reliability-based fatigue design of welded joints on aluminum high-speed vessels. *J Ship Res* 50:85–98
17. Liu PL, Lin HZ, Der Kiureghian A (1989) CalREL user manual. Department of Civil Engineering, University of California, Berkeley
18. Brady TF (2004) Global structural response measurement of SWIFT (HSV-2) from JLOTS and blue game rough water trials. NSWCCD-65-TR- 2004/33, Naval Surface Warfare Center, Carderock Division
19. Brady TF (2004) HSV-2 swift instrumentation and technical trials plan. NSWCCD-65-TR- 2004/18, Naval Surface Warfare Center, Carderock Division
20. Brady TF (2004) Wave impact loading response measurement and analysis for HSV-2 from JLOTS and blue game rough water trials. NSWCCD-65-TR- 2004/32, Naval Surface Warfare Center, Carderock Division
21. Downing SD, Socie DF (1982) Simple rainflow counting algorithms. *Int J Fatigue* 4:31–40